



This is the accepted manuscript made available via CHORUS. The article has been published as:

Obstruction of broken symmetries in topological flat bands

Penghao Zhu, Shi Feng, and Yuan-Ming Lu

Phys. Rev. B **111**, L161411 — Published 25 April 2025

DOI: 10.1103/PhysRevB.111.L161411

Obstruction to Broken Symmetries in Topological Flat Bands

Penghao Zhu, Shi Feng, and Yuan-Ming Lu
Department of Physics, The Ohio State University, Columbus, OH 43210, USA

Motivated by the abundance of symmetry breaking states in magic-angle twisted bilayer graphene and other two-dimensional materials, we study superconducting (SC) and charge orders in two-dimensional topological flat bands in the strong correlation regime. By relating the half-filled 2D topological flat bands to the surface states of 3D topological insulators in symmetry class AIII, we reveal the topological obstruction to the formation of gapped SC and inter-valley charge orders without intrinsic topological orders, in the presence of the anti-unitary particle-hole symmetry at half filling. This is a generalization of the Li-Haldane arguments for nodal superconductivity to strongly interacting electrons. In contrast to the $\mathbb{Z}$-valued obstruction derived from the non-interacting band topology, the topological obstruction of interacting electrons in half-filled flat bands has a $\mathbb{Z}_8$ classification, depending on the charge (valley) Chern number of the superconducting (inter-valley charge) orders. This is demonstrated by an interacting Hamiltonian for half-filled flat bands with a net Chern number $C = 4$, where superconductivity and $\mathbb{Z}_2$ topological order coexist in a gapped ground state with particle-hole symmetry.

Introduction.— Topological phases of matter are characterized by their robust properties stemming from the quantum entanglement of their ground states [1]. While topological phases cannot be distinguished and classified by local order parameters resulting from spontaneous symmetry breaking, there is a close relationship between topological phases and long-range orders. The presence of long-range orders facilitates the emergence of topological phases by establishing the topological gaps, as can be seen from the following examples: (i) Magnetic orders are crucial for quantum anomalous hall phases [2–4]; (ii) Superconducting orders are pertinent to topological superconductors hosting Majorana zero modes, where the Bogoliubov-de Gennes (BdG) quasiparticles exhibit nontrivial topology [5–8]; (iii) Gaps associated with charge orders, such as Peierls charge density waves in 1D, can result in topological insulators with quantized polarizations [9, 10]; (iv) Topological Mott insulators spontaneously break the spin rotational symmetry [11], facilitating the spin-orbit couplings needed for topological insulators[12–14]. With compelling evidence demonstrating the one-way influence of long-range orders on topological phases, it is natural to ask the following fundamental question: How can the topology affect the long-range order in the ground state?

One well-known example of such is the BCS-type superconductivity (SC) in a magnetic Weyl semimetal, where pairing order parameter between two Fermi surfaces (FSs) enclosing two Weyl points of opposite chirality must be nodal [15, 16]. Interestingly, there is a topological obstruction to a gapped/nodeless SC state due to the Chern number of paired electrons on the FSs. Inspired by this result, topological obstruction to gapped superconductors have been discussed for pairings between electrons in normal states with nontrivial $\mathbb{Z}_2$ topology [17], fragile topology [18, 19], and delicate topology [20]. Moreover, topologically obstructed gapless/nodal charge order has also been studied for electrons in topological bands with nonzero Chern numbers [21, 22]. The fundamental idea behind these works is to establish a connection between the vorticity of the order parameters and the topological invariants of electronic bands. As a result, the presence of nontrivial topological invariants indicates the existence of nonvanishing vorticities of the order parameters in momentum space, and thus zero points of the order parameters. These arguments rely on the mean-field picture by analyzing the geometry and topology of non-interacting Bloch wavefunctions, which breaks down in the presence of strong interactions. Therefore, a natural question is: do the topological obstruction to gapped SC and charge orders persist in strongly correlated systems? Besides bearing the theoretical importance, addressing this question is also helpful for understanding ordered phases in realistic materials, given that the topologically obstructed SC order and inter-valley coherent (IVC) order have been proposed to occur in flat bands of Moire systems based on band theory [19, 22, 23], where the interactions are strong compared to the small band width.

In this work, we study the SC/charge orders arising from half-filled electrons in 2D flat bands with nonzero charge/valley Chern numbers that will be defined later. By mapping these electronic states to the surface states of 3D interacting symmetry protected topological (SPT) phases, we show that the SC order and charge order cannot be symmetrically gapped out without developing topological orders due to the bulk topology of the 3D SPTs. This topological obstruction to gapped long-range orders can be viewed as a generalization of the Lieb-Schultz-Mattis type theorems [24, 25] to long-range ordered phases. Furthermore, we demonstrate that these topologically obstructed long-range orders have a $\mathbb{Z}_8$ classification, in contrast with the $\mathbb{Z}$ classification derived from the non-interacting band theory. To demonstrate the topological obstruction in correlated electrons, we construct an interacting Hamiltonian for a set of flat

bands with net Chern number $C = 4$, and numerically obtain a symmetrically gapped ground state, where SC long-range order and Z_2 topological order coexist.

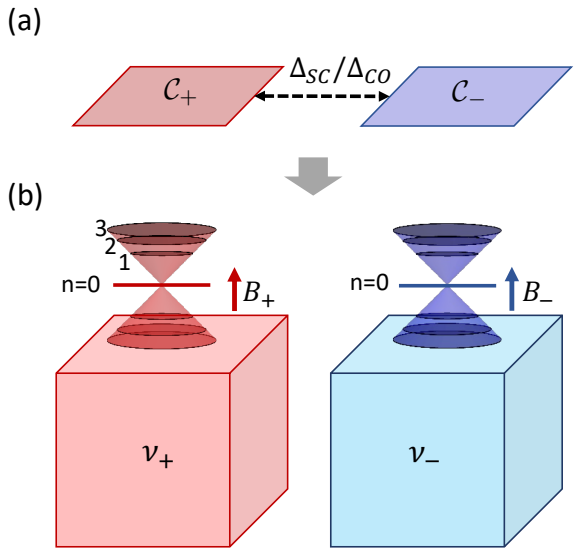


FIG. 1. (a)Illustration inter-valley SC and charge order for two flat Chern bands with Chern number $C_\pm$. Focusing on the $|C_\pm| = 1$ case, the two flat Chern bands can be mapped onto the zeroth LLs of the surface Dirac modes of 3D SPTs with bulk topological index $\nu_\pm$ shown in (b). The $0, 1, 2, 3$ in (b) labels different LLs.

Problem setup and symmetry.— As illustrated in Fig. 1(a), we start by considering two degenerate flat Chern bands (two "valleys"), $c^\dagger_{+,\mathbf{k}}$ and $c^\dagger_{-,\mathbf{k}}$, labelled by valley index $+$ and $-$. The Chern numbers of these two bands are respectively $\mathcal{C}_+$ and $\mathcal{C}_-$. We study the topological obstructions for *inter-valley* SC and charge orders in these half-filled flat bands, of which the order parameters are $\Delta_{\rm SC}(\mathbf{k}) = \langle c_{+,\mathbf{k}} c_{-,-\mathbf{k}}\rangle$ and $\Delta_{\rm CO}(\mathbf{k}) = \langle c^\dagger_{+,\mathbf{k}} c_{-,\mathbf{k}}\rangle$, respectively.

At half filling, by projecting the Hilbert space onto these two flat Chern bands, there will be an emergent, anti-unitary particle-hole (i.e. chiral) symmetry ($\hat{S}$), of which the representation is chosen to be

$$\hat{S} c^\dagger_{\pm,\mathbf{k}} \hat{S}^{-1} = \pm c_{\pm,\mathbf{k}}, \;\; \hat{S} i \hat{S}^{-1} = -i. \tag{1}$$

The above choice of chiral symmetry $\hat{S}$ forbids intra-valley terms such as $\tilde{\Delta}_1 c_{+,\mathbf{k}} c_{+,-\mathbf{k}} + h.c.$ and $\tilde{\Delta}_2 c^\dagger_{+,\mathbf{k}} c_{+,\mathbf{k}} + h.c.$, and automatically selects the inter-valley orders. If we choose the chiral symmetry to be the same in both valleys, any quadratic terms are forbidden by symmetry. This corresponds to a trivial case in which the symmetry inherently prohibits any possible symmetry-breaking orders. Note that although the chiral symmetry seems to impose strong constraints on interacting Hamiltonians, it is actually preserved for generic two-body interactions (up to a one-body term) at half filling and thus is relevant for realistic systems [26]. A detailed discussion of this point can be found in Supplementary Material (SM) [27]. Besides the chiral symmetry, we also consider the charge $U(1)$ and the valley $U(1)$ symmetries, denoted as $U_c(1)$ and $U_v(1)$, which respectively correspond to the conservation of the net charge and the charge difference between the $\pm$ valleys. Importantly, the SC and charge orders correspond to spontaneous breaking of $U_c(1)$ and $U_v(1)$, respectively. With these symmetries in mind, we can now concretely formulate the topological obstructions to inter-valley SC and charge orders as the following question:

- Starting with a half-filled interacting electron system with $U_c(1) \times U_v(1) \times Z_2^{\hat{S}}$ symmetries, after breaking either $U_c(1)$ or $U_v(1)$ symmetry, is there a gapped ground state of SC or charge order that preserves the remaining symmetries?

Applying the non-interacting band theory at the mean-field level, it can be proven that the net vorticity of $\Delta_{\rm SC}(\mathbf{k})$ ($\Delta_{\rm CO}(\mathbf{k})$), which is defined as $vort = (1/2\pi)\sum_{\rm vortex} \oint \partial_{\mathbf{k}} \arg \Delta_{\rm SC(CO)}(\mathbf{k})$, is determined by the Chern numbers of the two sectors through $vort = \mathcal{C}_+ + \mathcal{C}_-$ ($vort = \mathcal{C}_+ - \mathcal{C}_-$) [15, 16, 18–22]. A review of this Chern-vorticity theorem can be found in the SM [27]. When $vort$ is nonzero, there must be zero points of $\Delta_{\rm SC}(\mathbf{k})$ ($\Delta_{\rm CO}(\mathbf{k})$) in the momentum space. Consequently, the corresponding quadratic term $\Delta_{\rm SC}(\mathbf{k}) c^\dagger_{+,\mathbf{k}} c^\dagger_{-,-\mathbf{k}} + \text{H.c.}$ ($\Delta_{\rm CO}(\mathbf{k}) c^\dagger_{+,\mathbf{k}} c_{-,\mathbf{k}} + \text{H.c.}$), which is the only chiral symmetric SC pairing (charge order) term, cannot give rise to a full gap in the fermion spectrum. Equivalently, this means that there is no chiral symmetric, gapped ground state with SC or charge order. Note that the above Chern-vorticity theorem points to an integer($\mathbb{Z}$)-valued obstruction to gapped SC/charge order, since the net vorticity is $\mathbb{Z}$-valued.

Topological obstructions in strongly correlated systems.— In the strong correlation regime, however, the above proof for Chern-vorticity theorem based on the band theory breaks down, calling for a new approach to establish topological obstruction in interacting systems. To this end, we first focus on the simplest case where $|C_\pm| = 1$, and map the flat Chern bands onto the surface states of 3D class AIII fermionic topological insulators (i.e. 3D fermionic SPTs with $U(1) \times Z_2^{\hat{S}}$ symmetry) following the idea introduced in Ref. [26, 28]. Through this map, we can associate the topological obstruction for gapped SC/charge-ordered ground states to the bulk topology of the 3D SPT, because a nontrivial 3D bulk guarantees the surface, if preserving the bulk symmetries, to be either gapless or gapped with topological orders, no matter how strong the interactions are [29]. Therefore, the impossibility for a symmetric gapped 2D surface state without topological order leads to the the topological obstruction for gapped SC and charge orders of strongly interacting electrons in 2D flat bands, which

supersedes the Chern-vorticity theorem at the mean-field level.

To understand the above claims, let us first establish the map between 2D flat bands and surface states of 3D SPTs. In the non-interacting limit, a 3D class AIII SPT with bulk invariant $\nu \in \mathbb{Z}$ can host $|\nu|$ massless Dirac fermions on its surface. Focusing on $\nu = \pm 1$ cases, the massless surface modes can be depicted by Dirac Hamiltonian

$$h_{\nu=\pm 1} = \sum_{\mathbf{k}} \psi^\dagger_{\text{surf},\mathbf{k}} \hbar v (k_x \sigma_x \mp k_y \sigma_y) \psi_{\text{surf},\mathbf{k}} \tag{2}$$

where $\psi^\dagger_{\text{surf},\mathbf{k}} = (\psi^\dagger_{\text{surf},1,\mathbf{k}}, \psi^\dagger_{\text{surf},2,\mathbf{k}})$ and $\psi^\dagger_{\text{surf},l,\mathbf{k}}$ creates an electron with momentum $\mathbf{k}$ and orbital index $l = 1, 2$ on the surface; and $\sigma_{x,y,z}$ are Pauli matrices. $h_{\nu=\pm 1}$ preserves an anti-unitary particle-hole (chiral) symmetry $\hat{S}'$:

$$\hat{S}' \psi^\dagger_{\text{surf},l,\mathbf{k}} \hat{S}'^{-1} = (\sigma_z)_{ll'} \psi_{\text{surf},l',\mathbf{k}}, \;\; \hat{S}' i \hat{S}'^{-1} = -i. \tag{3}$$

Upon applying a magnetic field B as illustrated in Fig. 1(b), the surface Dirac mode develops Landau levels (LLs), the zeroth of which is pinned at zero energy due to the chiral symmetry. Several properties of the zeroth LL that are important for our following analysis, as we list below (see SM[27] for details): (i) The zeroth LL wave function is identical to a 2D lowest LL (LLL). (ii) The states on the zeroth LL, denoted as $d^\dagger_{\text{ZLL},n}$ where n labels the orbitals, transform under the chiral symmetry as $\hat{S}' d^\dagger_{\text{ZLL},n} \hat{S}'^{-1} = \text{sgn}(\nu)\text{sgn}(B) d_{\text{ZLL},n}$. (iii) the Chern number of the zeroth LL of is given by $\text{sgn}(B)$. Given point (i), mapping a flat Chern band to a surface zeroth LL is equivalent to mapping a flat Chern band to a 2D LLL. The map from a Chern band of Chern number $\mathcal{C}$ to a 2D LLL can be implemented by mapping each Bloch-Wannier state [30], which is localized along one direction but extended along the other direction, to the stripe-like LLL eigenstate in the Landau gauge. Specifically, the creation operator of a Bloch-Wannier state takes the form of

$$c^\dagger_{k_y,x_0} = \int d^2 r W_{k_y,x_0}(\mathbf{r}) \psi^\dagger_{\mathbf{r}}, \tag{4}$$

where $\psi^\dagger_{\mathbf{r}}$ creates an electron at position $\mathbf{r}$, and $W_{k_y,x_0}(\mathbf{r})$ is the Bloch-Wannier wave function centered at x_0 along x-direction. $W_{k_y,x_0}(\mathbf{r})$ can be generally derived by Fourier transforming the Bloch wave function $\Phi_{\mathbf{k}}(\mathbf{r})$ along x-direction: $W_{k_y,x_0}(\mathbf{r}) = \sum_{k_x} e^{-ik_x x_0} \Phi_{\mathbf{k}}(\mathbf{r})/\sqrt{N_x}$, where N_x is the number of unit cells along x-direction. Replacing $W_{k_y,x_0}(\mathbf{r})$ by the Gaussian function $\frac{1}{\sqrt{\pi^{1/2} L_y l_B}} e^{ik_y y} e^{-\left(x - \mathcal{C} k_y l_B^2\right)^2 / 2 l_B^2}$ maps the Bloch-Wannier state to a stripe-like state in LLL. Here, L_y is the linear size of the system along y-direction, $l_B = \sqrt{\hbar/eB}$ is the magnetic length, and $k_y = 2\pi n / L_y$ with n being an integer. Note that for the stripe-like LLL state, x_0 and k_y are both determined by the integer n in the range of $[1, eBL_xL_y/h]$, where L_x is the linear size of the system along x-direction and eBL_xL_y/h is the Landau degeneracy. Hereafter, we denote the creation/annihilation operator of stripe-like LLL state by $c^\dagger_n / c_n$.

After establishing the map, we are now ready to discuss the topological obstructions for the SC and charge orders. As depicted in Fig. 1(b), we map the flat Chern bands with Chern number $C_\pm$ to the surface states of 3D SPTs with bulk topological invariants $\nu_\pm$ and subjected to magnetic field $B_\pm$. Meanwhile, we map the 2D chiral symmetry $\hat{S}$ to the surface symmetry $\hat{S}'$, which requires $\text{sgn}(\nu_+)\text{sgn}(B_+) = -\text{sgn}(\nu_-)\text{sgn}(B_-) = +1$ according to aforementioned property (ii). Note that although $\hat{S}'$ originates from a locality-preserving (on-site) symmetry of the 3D system, due to the nontrivial bulk topology of the 3D SPT, it is mapped to a nonlocal symmetry $\hat{S}$ in 2D. For the SC order where $U_c(1)$ is spontaneously broken, $U_v(1) \times Z_2^{\hat{S}'}$ symmetry leads to a 3D bulk characterized by a topological invariant $\nu_v = \nu_+ - \nu_-$. Consequently, when $\nu_+ = -\nu_- = +1$ and thus $B_+ = B_-$, we have $\nu_v = 2$ indicating that the surface cannot be symmetrically gapped out unless developing a topological order. This directly implies that when the two flat Chern bands have $\mathcal{C}_+ = \mathcal{C}_- = +1$ [c.f. point (iii)], there cannot be symmetric, gapped SC phase without topological order, i.e., the SC order is topologically obstructed. For the charge order where $U_v(1)$ is spontaneously broken, the 3D bulk will be characterized by a topological invariant $\nu_c = \nu_+ + \nu_-$ with $U_c(1) \times Z_2^{\hat{S}'}$ symmetry. Similarly, when $\nu_+ = \nu_- = +1$ and thus $B_+ = -B_-$, the ν_c is 2 which indicates that when $\mathcal{C}_+ = -\mathcal{C}_- = 1$, the charge order is topologically obstructed.

The above arguments for topological obstructions is valid independent of the form and the strength of interactions we consider, as long as the $U(1) \times Z_2^{\hat{S}'}$ symmetry is preserved. Naively, the interacting topological obstruction should be consistent with the Chern-vorticity theorem derived from the band theory, corresponding to a $\mathbb{Z}$ classification associated with the valley/charge Chern number $\mathcal{C}_{c/v} \in \mathbb{Z}$. However, as we will discuss below, strong interactions give rise to a $\mathbb{Z}_8$ topological obstruction, in contrast to the $\mathbb{Z}$ obstruction at the non-interacting level. Before that, we note that flat Chern bands generally do not have a smooth quantum geometry as in LLL, and thus during the map discussed above the information about the quantum geometry is inevitably lost. However, the presence of obstructions does not depend on the quantum geometry as long as the emergent chiral is (approximately) preserved – Symmetry-allowed terms can always be added to deform the zeroth Landau level of the surface Dirac modes, resulting in non-ideal quantum geometry, and the bulk topology will continue to impose constraints on the surface states, and consequently, on the associated flat Chern bands.

$\mathbb{Z}_8$ classification of the topological obstruction.— In the

strongly interacting regime, it is known that the classification of the 3D fermion SPT of class AIII reduces from $\mathbb{Z}$ to $\mathbb{Z}_8$[29]. This means that the surface states can be gapped out symmetrically without developing any topological orders when $\nu = 8$. Consequently, if the net Chern numbers in $\pm$ valleys are $\mathcal{C}_+ = \mathcal{C}_- = 4$ ($\mathcal{C}_+ = -\mathcal{C}_- = 4$)[31], the SC (charge) order is no longer topologically obstructed. Since the chiral symmetry is nonlocal in 2D flat Chern bands, it is difficult to explicitly write down a chiral symmetric ground state. The simplest way to understand the $\mathbb{Z}_8$ classification is to the vortex proliferation argument for 3D TI surface discussed in Ref. [29]. For pedagogical purposes, we briefly review it here and then apply it to the SC and charge orders.

Let us first consider the charge order where the 3D bulk invariants associated with $U_c(1) \times Z_2^{\hat{S}'}$ symmetry are $\nu_+ = \nu_- = +4$ and thus $\nu_c = 8$, corresponding to flat Chern bands with $\mathcal{C}_+ = -\mathcal{C}_- = +4$. In this case, there are eight Dirac modes on the surface, each of which is described by $h_{\nu=+1}$ in Eq. (2). If breaking the $U_c(1)$ symmetry protecting the bulk topology, the surface states can be gapped out by the following pairing term

$$h_1 = \sum_{j,\mathbf{k}} (\psi_{\text{surf},j,\mathbf{k}})^T \, i\Delta\sigma_y \psi_{\text{surf},j,\mathbf{k}} + h.c., \tag{5}$$

where $j = (\pm, m)$ with valley index $\pm$ and flavor index $m = 1, 2, 3, 4$, and Δ is the pairing order parameter. Though breaking the $U_c(1)$ symmetry, this term preserves the chiral symmetry $\hat{S}'$. Strong interactions can lead to quantum fluctuations of Δ, and restore $U_c(1)$ symmetry by proliferating vortices of the SC order parameter Δ. To understand the vortex porliferation process, we need to examine the zero-energy modes in each vortex. Each surface Dirac mode produces a Majorana zero mode (MZM), γ_n, in one vortex [32] that transforms trivially under the chiral symmetry: $\hat{S}'\gamma_n\hat{S}'^{-1} = \gamma_n$. Consequently, eight surface Dirac modes leads to eight MZMs in each vortex, which can be gapped out symmetrically [33]. Given that the symmetrically gapped vortex state is a linear combination of states with even fermion parity, each vortex is a bosonic excitation [27, 29] and consequently we can condense the vortices to restore $U_c(1)$ symmetry, leaving the surface to be a trivial, symmetric, gapped state. The same argument applies to four copies of topologically obstructed SC orders with $\nu_v = 8$, and we discuss the details in SM [27].

Following a similar argument, one can show that the surface can be symmetrically gapped out and develop a $\mathbb{Z}_2$ topological order when $\nu = 4$ [29]. This suggests that a symmetric, gapped SC (charge) order in flat Chern bands with $\mathcal{C}_+ = \mathcal{C}_- = +2$ ($\mathcal{C}_+ = -\mathcal{C}_- = +2$) must coexist with a topological order. Below we construct such an interacting Hamiltonian and identify its symmetric ground state with coexisting SC and topological orders.

Symmetrically gapped SC state with coexisting topological order.— In this section we construct a gapped SC state coexisting with topological order, formulated using Wannier-Bloch states of the flat Chern bands. To see this, we consider two flat bands labelled by index $j = 1, 2$ in each of the $\pm$ valleys, each with a Chern number of $+1$, corresponding to $\mathcal{C}_+ = \mathcal{C}_- = +2$. As discussed previously, a mean-field pairing term $H_{\text{pair}} = \sum_{\mathbf{k},j=1,2}(\Delta_{\text{SC}}(\mathbf{k})c^\dagger_{+,j,\mathbf{k}}c^\dagger_{-,j,-\mathbf{k}} + h.c.)$ cannot gap out the systems because $\Delta_{\text{SC}}(\mathbf{k})$ must vanish at certain momenta. Other interactions are needed to achieve a gapped superconductor, and we consider the hard-core interaction

$$H_{\text{int}} = \int d^2r d^2r' V(\mathbf{r}-\mathbf{r}')\psi^\dagger_{+,1,\mathbf{r}}\psi^\dagger_{-,1,\mathbf{r}'}\psi_{+,2,\mathbf{r}'}\psi_{-,2,\mathbf{r}} + h.c. \tag{6}$$

where $V(\mathbf{r}-\mathbf{r}') = V_0\delta(\mathbf{r}-\mathbf{r}')$ and $\psi^\dagger_{\pm,m,\mathbf{k}}$ creates fermions in the m-th flavor of valley $\pm$. H_{int} preserves the full symmetry $U_c(1)\times U_v(1)\times\hat{S}$, though $U_c(1)$ is explicitly broken by H_{pair}. Projecting the Hilbert space onto the flat Chern bands, the fermion creation operator can be expanded by a linear combination of Bloch-Wannier states:

$$\psi^\dagger_{\pm,m,\mathbf{r}} \approx \sum_{(k_y,x_0)} W^\star_{\pm,m,k_y,x_0}(\mathbf{r})c^\dagger_{k_y,x_0}. \tag{7}$$

Without loss of generality, we use the LLL form $W_{\pm,m,k_y,x_0}(\mathbf{r}) = e^{ik_y y}\frac{1}{\sqrt{\pi^{1/2}L_y l_B}}e^{-\left(x-\mathcal{C}_\pm k_y l_B^2\right)^2/2l_B^2}$, for which the label (k_y, x_0) can be combined into an integer index n as discussed previously. Substituting Eq. (7) into Eq. (6), we have

$$H_{\text{int}} = \sum_{l,p,q}\tilde{V}_{p,q}c^\dagger_{+,1,l+p}c^\dagger_{-,1,l-p}c_{+,2,l-q}c_{-,2,l+q} + h.c., \tag{8}$$

where $\tilde{V}_{p,q} = g\kappa\exp\left\{-\kappa^2(p^2+q^2)\right\}$ with $\kappa = 2\pi l_B/L_y$ and $g = V_0/[(2\pi)^{3/2}l_B^2]$. l, p, q take half integer values, and $l \pm q$ and $l \pm p$ are integers labelling the center of the stripe-like states along x-direction. From Eq. (6) to Eq. (8), we reduce a 2D problem into a 1D problem by rewriting the two-body potential in terms of stripe-like states in LLL [34, 35]. Details can be found in SM [27].

Let us first consider the thin cylinder limit, where x-direction is open, and y-direction is periodic with $L_y \ll l_B$. In this limit, κ is large, and Eq. (8) is dominated by its leading term

$$\tilde{H}_{\text{int}} = g\kappa\sum_l c^\dagger_{+,1,l}c^\dagger_{-,1,l}c_{+,2,l}c_{-,2,l} + h.c., \tag{9}$$

which has a ground state at half-filling with energy $E_0 = -g\kappa$:

$$|G_0\rangle = \prod_l (c^\dagger_{+,1,l}c^\dagger_{-,1,l} - c^\dagger_{+,2,l}c^\dagger_{-,2,l})|0\rangle. \tag{10}$$

Since $\hat{S}|0\rangle = c^\dagger_{+,1,l}c^\dagger_{-,1,l}c^\dagger_{+,2,l}c^\dagger_{-,2,l}|0\rangle$, it is straightforward to verify that $|G_0\rangle$ preserves $U_c(1) \times U_v(1) \times \hat{S}$

symmetry. Assuming weak pairing, we can treat H_{pair} as a perturbation to $\tilde{H}_{\text{int}}$, and a gapped SC state can be obtained using non-degenerate perturbation theory:

$$|G\rangle = |G_0\rangle - \sum_{\text{exc}} \frac{\langle \text{exc}|H_{\text{pair}}|G_0\rangle}{E_{\text{exc}} + g\kappa}|\text{exc}\rangle + \cdots \tag{11}$$

In the thin cylinder limit, all excited states $|\text{exc}\rangle$ with non-vanishing coefficient in Eq. (11) must have energy $E_{\text{exc}} = 0$ and thus have excitation energy $E_{\text{exc}} - E_0 = g\kappa$. This is because H_{pairing} can only take $|G_0\rangle$ into excited states that are not half-filling, and all such states are eigenstates of $\tilde{H}_{\text{int}}$ with eigenvalue 0. Importantly, $|G\rangle$ is $U_v(1) \times Z_2^{\hat{S}}$ symmetric because H_{pair}, $|G_0\rangle$, and $\sum_{\text{exc}} |\text{exc}\rangle\langle\text{exc}| = \mathbb{1} - |G_0\rangle\langle G_0|$ all are $U_v(1) \times \hat{S}$ symmetric [27]. Since H_{pair} is only a perturbation and the energy gap of excitations is dominated by $g\kappa$, the fact that $\Delta(\mathbf{k})$ vanishes at some momenta will not affect the gapped nature of the ground state.

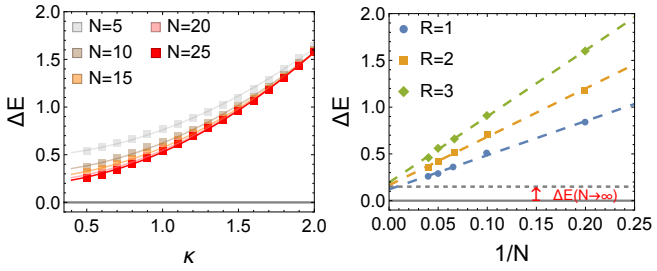


FIG. 2. Energy Gap ΔE (in unit of g) of Eq. (9) for different sizes (N) and geometries. (left) Gaps under different κ and different N, and their fittings $\Delta E(\kappa; N)$ by quadratic functions. (right) Finite size scaling of gaps as a function of $1/N$, under fixed aspect rations ($R = 1, 2, 3$). Data points in markers are obtained by DMRG under open boundary condition, with the maximal bond dimension $d = 800$ and truncation errors $\epsilon \sim 10^{-7}$. Details can be found in SM [27].

Based on the $\mathbb{Z}_8$ classification discussed previously, a gapped, symmetric $|G\rangle$ in the thin cylinder limit indicates a ground state where SC order and topological order coexist, provided the gap does not close as we increase L_y (decrease κ) and the system size approaches the 2D limit. Next, we provide numerical evidence that the gap will indeed persist in a 2D cylinder geometry. Specifically, we perform density matrix renormalization group (DMRG) calculations [27, 36] for the effective 1D model (8) for various $\kappa = 2\pi l_b/L_y$ and system sizes $N = L_x L_y$. As κ decreases for systems of different sizes, no level crossing has been observed. As shown in Fig. 2(left), with fixed system size N, the gap will saturate to a finite value as κ decreases. This saturation value of the energy gap converges as we increase the system size. Moreover, we present the finite-size scaling of the energy gap for systems with fixed aspect ratios $R \equiv L_x/L_y = 1, 2, 3$ in Fig. 2(right). This amounts to extrapolating to the true 2D limit with $\kappa \to 0$, $L_x, L_y \sim O(\kappa^{-1}) = O(\sqrt{N})$. The energy gap of systems with different R converges to the same finite value in the thermodynamic limit, i.e., $\Delta E(1/N \to 0) \sim 0.15g$, as marked out by the gray dashed horizontal line in Fig. 2(right). These numerical evidences strongly suggest that no phase transition occurs as the system evolves from a thin cylinder to a 2D cylinder geometry. Consequently, as we increase L_y, $|G\rangle$ will remain a gapped, symmetric ground state with SC order in 2D. As argued previously, such a gapped symmetric state with $\nu_v = 4$ must also exhibit topological orders, in addition to SC order. Therefore we reach a symmetric gapped ground state with coexisting long-range and topological orders.

Discussions— In this work, we have established an LSM-type topological obstruction to trivially gapped SC and charge orders in strongly correlated flat Chern bands at half filling. Our results reveal an intriguing connection between long-range orders and topological orders, i.e., the presence of certain symmetric, gapped long-range orders is necessarily accompanied by topological orders. Importantly, the flat Chern bands discussed in this work can be realized either in 2D moire systems [22, 37–39] and/or on the Fermi surface of 3D topological semimetals such as Weyl semimetals [16, 40, 41], for which the $U_v(1)$ symmetry are indeed realized as a valley-$U(1)$ symmetry. We emphasize that the emergent chiral symmetry, arising from projecting the Hilbert space onto flat bands, is vital for the topological obstruction. If this symmetry is broken, a gapped incommensurate valley coherence (IVC) order can emerge. In twisted bilayer-graphenes, the finite width and nontrivial dispersion of the flat Chern bands will generally break the emergent chiral symmetry. As a result, incommensurate Kekulé orders have been theoretically proposed [42–44] experimentally confirmed [45]. The emergent chiral symmetry of flat Chern bands in real materials should be considered as an approximate symmetry. The closer the flat Chern bands resemble the LLL, the more accurate this approximation becomes, since we know that a chiral symmetry can emerge when projecting onto the LLL. Therefore, we expect the topological obstruction discussed in our paper would be more influential in systems with flat Chern bands that are significantly similar to LLL, e.g. in twisted $MoTe_2$ homobilayers [46–52], where the breaking of the emergent chiral symmetry is expected to be weaker and thus it is harder to have a trivially gapped IVC order. Indeed, the authors of Ref. [51] also highlighted the approximate emergent chiral symmetry when discussing the physical responses of the proposed composite Fermi liquid in twisted $MoTe_2$. Moreover, the even-denominator $\nu = 3/2$ fractional spin Chern insulator has already been observed in experiments [52], of which the physics is closely related to the half-filled flat Chern bands and the approximate emergent chiral symmetry discussed in our work. We hope our theory can

provide new insights and lead to further investigations to understand this experimentally observed phase. Besides the twisted $MoTe_2$, periodically strained monolayer graphene has also been proposed to have flat Chern bands that closely resembles the LLL [53], where our theory can be applied.

Looking forward, two questions naturally arise from this work: (i) can one explicitly construct a featureless and gapped ground state (w/o topological orders) for the $\nu = 8$ case, e.g. in the context of SC orders in topological flat bands with $\mathcal{C}_+ = \mathcal{C}_- = 4$? (ii) Can the topological obstructions discussed here be generalized to correlated flat bands of other symmetry classes, such as class DIII and class CII? We leave these intriguing questions for future works.

Acknowledgments: We thank Jiabin Yu, Ya-Hui Zhang, and Rui-Xing Zhang for their insightful discussions. We also extend our gratitude to Siddharth A. Parameswaran and Nemin Wei for their valuable discussions on materials. This research was primarily supported by the Center for Emergent Materials, an NSF MRSEC, under award number DMR-2011876.

REFERENCES

[1] B. Zeng, X. Chen, D.-L. Zhou, and X.-G. Wen, Gapped quantum systems and entanglement area law, in *Quantum Information Meets Quantum Matter: From Quantum Entanglement to Topological Phases of Many-Body Systems* (Springer New York, New York, NY, 2019) pp. 115–153.

[2] F. D. M. Haldane, Model for a quantum hall effect without landau levels: Condensed-matter realization of the "parity anomaly", Phys. Rev. Lett. **61**, 2015 (1988).

[3] C.-Z. Chang, J. Zhang, X. Feng, J. Shen, Z. Zhang, M. Guo, K. Li, Y. Ou, P. Wei, L.-L. Wang, Z.-Q. Ji, Y. Feng, S. Ji, X. Chen, J. Jia, X. Dai, Z. Fang, S.-C. Zhang, K. He, Y. Wang, L. Lu, X.-C. Ma, and Q.-K. Xue, Experimental observation of the quantum anomalous hall effect in a magnetic topological insulator, Science **340**, 167 (2013), https://www.science.org/doi/pdf/10.1126/science.1234414.

[4] Y. Deng, Y. Yu, M. Z. Shi, Z. Guo, Z. Xu, J. Wang, X. H. Chen, and Y. Zhang, Quantum anomalous hall effect in intrinsic magnetic topological insulator $mnbi_2te_4$, Science **367**, 895 (2020), https://www.science.org/doi/pdf/10.1126/science.aax8156.

[5] A. P. Schnyder, S. Ryu, A. Furusaki, and A. W. W. Ludwig, Classification of topological insulators and superconductors in three spatial dimensions, Phys. Rev. B **78**, 195125 (2008).

[6] A. Kitaev, Periodic table for topological insulators and superconductors, in *AIP conference proceedings*, Vol. 1134 (American Institute of Physics, 2009) pp. 22–30.

[7] X.-L. Qi and S.-C. Zhang, Topological insulators and superconductors, Rev. Mod. Phys. **83**, 1057 (2011).

[8] M. Sato and Y. Ando, Topological superconductors: a review, Reports on Progress in Physics **80**, 076501 (2017).

[9] W. P. Su, J. R. Schrieffer, and A. J. Heeger, Solitons in polyacetylene, Phys. Rev. Lett. **42**, 1698 (1979).

[10] J. K. Asbóth, L. Oroszlány, and A. Pályi, A short course on topological insulators, Lecture notes in physics **919**, 166 (2016).

[11] S. Raghu, X.-L. Qi, C. Honerkamp, and S.-C. Zhang, Topological mott insulators, Phys. Rev. Lett. **100**, 156401 (2008).

[12] M. Z. Hasan and C. L. Kane, Colloquium: Topological insulators, Rev. Mod. Phys. **82**, 3045 (2010).

[13] M. Z. Hasan and J. E. Moore, Three-dimensional topological insulators, Annual Review of Condensed Matter Physics **2**, 55 (2011).

[14] X.-L. Qi and S.-C. Zhang, Topological insulators and superconductors, Rev. Mod. Phys. **83**, 1057 (2011).

[15] S. Murakami and N. Nagaosa, Berry phase in magnetic superconductors, Phys. Rev. Lett. **90**, 057002 (2003).

[16] Y. Li and F. D. M. Haldane, Topological nodal cooper pairing in doped weyl metals, Phys. Rev. Lett. **120**, 067003 (2018).

[17] C. Sun and Y. Li, $\mathbb{Z}_2$ topologically obstructed superconducting order, arXiv preprint arXiv:2009.07263 (2020).

[18] J. Yu, Y.-A. Chen, and S. Das Sarma, Euler-obstructed cooper pairing: Nodal superconductivity and hinge majorana zero modes, Phys. Rev. B **105**, 104515 (2022).

[19] J. Yu, M. Xie, F. Wu, and S. Das Sarma, Euler-obstructed nematic nodal superconductivity in twisted bilayer graphene, Phys. Rev. B **107**, L201106 (2023).

[20] P. Zhu and R.-X. Zhang, Dipole-obstructed cooper pairing: Theory and application to $j = 3/2$ superconductors, arXiv preprint arXiv:2405.00091 (2023).

[21] E. Bobrow, C. Sun, and Y. Li, Monopole charge density wave states in weyl semimetals, Phys. Rev. Res. **2**, 012078 (2020).

[22] N. Bultinck, S. Chatterjee, and M. P. Zaletel, Mechanism for anomalous hall ferromagnetism in twisted bilayer graphene, Phys. Rev. Lett. **124**, 166601 (2020).

[23] Y.-J. Wang, G.-D. Zhou, S.-Y. Peng, B. Lian, and Z.-D. Song, Molecular pairing in twisted bilayer graphene superconductivity, arXiv preprint arXiv:2402.00869 (2024).

[24] E. Lieb, T. Schultz, and D. Mattis, Two soluble models of an antiferromagnetic chain, Annals of Physics **16**, 407 (1961).

[25] M. Oshikawa, Commensurability, excitation gap, and topology in quantum many-particle systems on a periodic lattice, Phys. Rev. Lett. **84**, 1535 (2000).

[26] C. Wang and T. Senthil, Half-filled landau level, topological insulator surfaces, and three-dimensional quantum spin liquids, Phys. Rev. B **93**, 085110 (2016).

[27] See the Supplemental Material, for more details about...

[28] A. C. Potter, C. Wang, M. A. Metlitski, and A. Vishwanath, Realizing topological surface states in a lower-dimensional flat band, Phys. Rev. B **96**, 235114 (2017).

[29] C. Wang and T. Senthil, Interacting fermionic topological insulators/superconductors in three dimensions, Phys. Rev. B **89**, 195124 (2014).

[30] X.-L. Qi, Generic wave-function description of fractional quantum anomalous hall states and fractional topological insulators, Phys. Rev. Lett. **107**, 126803 (2011).

[31] This is equivalent to stacking four copies of those depicted in Fig. 1.

[32] L. Fu and C. L. Kane, Superconducting proximity effect and majorana fermions at the surface of a topological

insulator, Phys. Rev. Lett. **100**, 096407 (2008).
[33] L. Fidkowski and A. Kitaev, Effects of interactions on the topological classification of free fermion systems, Phys. Rev. B **81**, 134509 (2010).
[34] D.-H. Lee and J. M. Leinaas, Mott insulators without symmetry breaking, Phys. Rev. Lett. **92**, 096401 (2004).
[35] A. Seidel, H. Fu, D.-H. Lee, J. M. Leinaas, and J. Moore, Incompressible quantum liquids and new conservation laws, Phys. Rev. Lett. **95**, 266405 (2005).
[36] M. Fishman, S. R. White, and E. M. Stoudenmire, The ITensor Software Library for Tensor Network Calculations, SciPost Phys. Codebases , 4 (2022).
[37] Y.-H. Zhang, D. Mao, Y. Cao, P. Jarillo-Herrero, and T. Senthil, Nearly flat chern bands in moiré superlattices, Phys. Rev. B **99**, 075127 (2019).
[38] G. Chen, A. L. Sharpe, E. J. Fox, Y.-H. Zhang, S. Wang, L. Jiang, B. Lyu, H. Li, K. Watanabe, T. Taniguchi, *et al.*, Tunable correlated chern insulator and ferromagnetism in a moiré superlattice, Nature **579**, 56 (2020).
[39] M. Serlin, C. Tschirhart, H. Polshyn, Y. Zhang, J. Zhu, K. Watanabe, T. Taniguchi, L. Balents, and A. Young, Intrinsic quantized anomalous hall effect in a moiré heterostructure, Science **367**, 900 (2020).
[40] N. P. Armitage, E. J. Mele, and A. Vishwanath, Weyl and dirac semimetals in three-dimensional solids, Rev. Mod. Phys. **90**, 015001 (2018).
[41] B. Q. Lv, T. Qian, and H. Ding, Experimental perspective on three-dimensional topological semimetals, Rev. Mod. Phys. **93**, 025002 (2021).
[42] Y. H. Kwan, G. Wagner, T. Soejima, M. P. Zaletel, S. H. Simon, S. A. Parameswaran, and N. Bultinck, Kekulé spiral order at all nonzero integer fillings in twisted bilayer graphene, Phys. Rev. X **11**, 041063 (2021).
[43] Z. Wang, Y. H. Kwan, G. Wagner, S. H. Simon, N. Bultinck, and S. Parameswaran, Chern-textured exciton insulators with valley spiral order in moir\'e materials, arXiv preprint arXiv:2406.15342 (2024).
[44] Y. H. Kwan, Z. Wang, G. Wagner, S. H. Simon, S. Parameswaran, and N. Bultinck, Textured exciton insulators, arXiv preprint arXiv:2406.15343 (2024).
[45] K. P. Nuckolls, R. L. Lee, M. Oh, D. Wong, T. Soejima, J. P. Hong, D. Călugăru, J. Herzog-Arbeitman, B. A. Bernevig, K. Watanabe, *et al.*, Quantum textures of the many-body wavefunctions in magic-angle graphene, Nature **620**, 525 (2023).
[46] F. Wu, T. Lovorn, E. Tutuc, I. Martin, and A. H. MacDonald, Topological insulators in twisted transition metal dichalcogenide homobilayers, Phys. Rev. Lett. **122**, 086402 (2019).
[47] T. Devakul, V. Crépel, Y. Zhang, and L. Fu, Magic in twisted transition metal dichalcogenide bilayers, Nature communications **12**, 6730 (2021).
[48] J. Dong, J. Wang, P. J. Ledwith, A. Vishwanath, and D. E. Parker, Composite fermi liquid at zero magnetic field in twisted mote$_2$, Phys. Rev. Lett. **131**, 136502 (2023).
[49] J. Cai, E. Anderson, C. Wang, X. Zhang, X. Liu, W. Holtzmann, Y. Zhang, F. Fan, T. Taniguchi, K. Watanabe, *et al.*, Signatures of fractional quantum anomalous hall states in twisted mote2, Nature **622**, 63 (2023).
[50] Y. Zeng, Z. Xia, K. Kang, J. Zhu, P. Knüppel, C. Vaswani, K. Watanabe, T. Taniguchi, K. F. Mak, and J. Shan, Thermodynamic evidence of fractional chern insulator in moiré mote2, Nature **622**, 69 (2023).
[51] V. Crépel, N. Regnault, and R. Queiroz, Chiral limit and origin of topological flat bands in twisted transition metal dichalcogenide homobilayers, Communications Physics **7**, 146 (2024).
[52] K. Kang, B. Shen, Y. Qiu, K. Watanabe, T. Taniguchi, J. Shan, and K. F. Mak, Observation of the fractional quantum spin hall effect in moir\'e mote2, arXiv preprint arXiv:2402.03294 (2024).
[53] Q. Gao, J. Dong, P. Ledwith, D. Parker, and E. Khalaf, Untwisting moiré physics: Almost ideal bands and fractional chern insulators in periodically strained monolayer graphene, Phys. Rev. Lett. **131**, 096401 (2023).